Journal of Micromechanics and Microengineering

Position-dependent mass responsivity of silicon MEMS cantilevers excited in the fundamental, two-dimensional roof tile-shaped mode

OPEN ACCESS
IOP Publishing
Journal of Micromechanics and Microengineering
J. Micromech. Microeng. **29** (2019) 045009 (7pp)
https://doi.org/10.1088/1361-6439/ab062a

Position-dependent mass responsivity of silicon MEMS cantilevers excited in the fundamental, two-dimensional roof tile-shaped mode

F Patocka[1,2,3], M Schneider[1], N Dörr[2], C Schneidhofer[2] and U Schmid[1]

[1] Institute of Sensor and Actuator Systems, TU Wien, Gußhausstraße 27-29, 1040 Vienna, Austria
[2] Austrian Centre of Competence for Tribology, AC2T research GmbH, Viktor-Kaplan-Straße 2, 2700 Wr. Neustadt, Austria

E-mail: florian.patocka@tuwien.ac.at (F Patocka)

Received 12 November 2018, revised 29 January 2019
Accepted for publication 11 February 2019
Published 28 February 2019

Abstract

The potential of a special class of eigenmodes of microcantilevers, the so-called roof tile-shaped modes, is investigated for resonant mass sensing. Due to the 2D shape of vibration, the mass responsivity (resonance frequency shift per unit mass change) of these modes depends on the position along the length and width of the cantilever. This is in contrast to the commonly used 1D eigenmodes, where the mass responsivity is only dependent on one spatial variable. We mapped the position-dependent mass responsivity of the fundamental roof tile-shaped mode by placing silicon dioxide microbeads as test mass on defined positions across the cantilever surface and measuring the corresponding shift in resonance frequency. The results show very good agreement with finite element analyses and are used to verify an analytic expression for the position-dependent mass responsivity. This expression allows for the calculation of the mass responsivity of an arbitrary point on the cantilever surface. A mass responsivity of 24 Hz ng^{-1} was found at the point of maximum oscillation amplitude at the free end of the cantilever, which rapidly decreases towards the nodal lines of the vibration. The 2D spatial distribution of the mass responsivity is discussed in this paper, which has to be considered in the design of high precision resonant mass sensors when targeting the roof tile-shaped mode. Since the accuracy in mass determination relies on the precise knowledge of the added mass position, the maximum error due to limited spatial accuracy is determined and the mid-section of the free end is identified to be the most suitable position on the cantilever surface for mass detection.

Keywords: MEMS, mass sensor, microcantilever, mass responsivity, resonance frequency

(Some figures may appear in colour only in the online journal)

[3] Author to whom any correspondence should be addressed.

1. Introduction

The use of resonantly excited microelectromechanical systems (MEMS) cantilevers as mass sensors was proposed about two decades ago (Cleveland *et al* 1993). The working principle is based on the dependence of the cantilevers resonance frequency on the total oscillating mass. By functionalizing the surface of the cantilever it is possible to promote the adsorption of specific substances, what allows for the detection of ultralow additional mass values down to the pg-level (Johnson and Mutharasan 2012). The resulting shift of the resonance frequency can be used to deduce the accumulated mass, which makes this sensor principle useful for a wide field of applications, ranging from biochemical analysis (Buchapudi *et al* 2011) to the detection of micro- and nano-sized particles (Wasisto *et al* 2013). Most studies utilize the flexural out-of-plane mode, which is well suited for mass sensing in vacuum and air. In liquids, however, the cantilever experiences high damping by the surrounding fluid what substantially deteriorates its mass sensing performance (Cox *et al* 2012). To circumvent this problem, higher order out-of-plane modes or different mode shapes, such as the in-plane mode, can be used for measurements in liquids (Dufour *et al* 2007, Van Eysden and Sader 2007). In the past, the application of the so-called *roof tile-shaped modes* for sensor applications was proposed (Kucera *et al* 2014). This special type of flexural mode has a 2D shape of vibration and shows superior performance (i.e. low damping) in liquid environments, resulting in quality factors of about 200 in water at resonance frequencies of approximately 300 kHz. This class of modes is therefore well-suited for mass sensing applications in a fluid environment. Pfusterschmied *et al* studied the potential of piezoelectrically excited resonators for viscosity and density sensing of fluids, using the roof tile-shaped modes (Pfusterschmied *et al* 2015, 2017). Recently, we showed the detection of ferrous particles in fluids using this class of modes, by monitoring the resonance frequency shift of a highly-integrated MEMS sensor (Patocka *et al* 2018). For the in-depth investigation of such mass measurements in liquid environments, a theoretical framework to connect the accumulated mass and the resonance frequency shift of the sensor is needed.

In this work, we map the spatial distribution of the mass responsivity $\mathcal{R} = \Delta\Omega/\Delta m$ (resonance frequency shift $\Delta\Omega$ per mass change Δm) of the fundamental roof tile-shaped mode across the cantilever surface. Because we are interested in investigating the validity of extending the analytical framework of the flexural out-of-plane modes to 2D modes, we conducted these experiments in vacuum to cancel out any viscous effects. The position dependency of the mass responsivity is used to determine the mass change from the mass sensor output signal, i.e. the resonance frequency shift. An earlier study investigated the performance of the roof tile-shaped mode for immunosensing, but did not consider the position-dependent mass responsivity of such modes (Oliver *et al* 2012). Due to the 2D mode shape, the mass responsivity depends on the position of the additional mass along the width and length of the resonator. This is in contrast to the out-of-plane mode, where $\mathcal{R}$ solely depends on the position along the cantilever axis (Dohn *et al* 2005). We performed these investigations by adding a small test mass in form of a spherical silicon dioxide microbead on predefined positions on the surface, thus ensuring a point-like connection, and subsequently measuring the resulting resonance frequency shift. Repeating this procedure, it is possible to map the mass responsivity across the cantilever surface. The latter measurements are evaluated against both finite element analyses (FEA) and an analytical expression, which is the extension of the analytical framework of the 1D modes to the 2D modes used in this study. Finally, the consequences for the design of resonant mass sensors, targeting the fundamental roof tile-shaped mode, are discussed. This work lays the foundation for the in-depth investigation of mass measurements in liquid environments using the class of roof tile-shaped modes of MEMS-cantilevers.

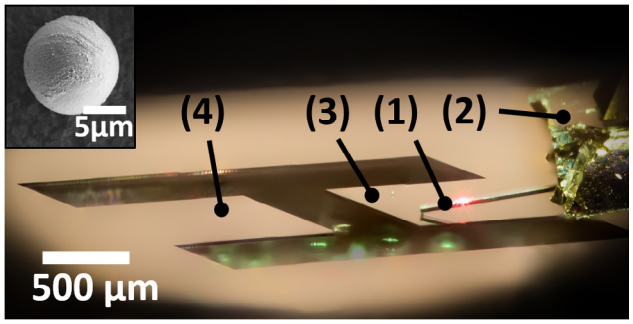

Figure 1. Confocal micrograph of the microcantilever used for the experiments. An AFM cantilever (1), fixed to the AFM probe body (2) is used to transfer a silicon oxide microbead (inset) to a $1000 \times 1000 \times 20\ \mu m^3$ silicon cantilever (3). An identical cantilever (4) is used as a reference during measurements to cancel out any parasitic temperature effects.

2. Materials and experimental details

Commercially available silicon dioxide microbeads[4] with a diameter of approximately 10 μm were used as test masses. Since the mass of the used bead directly affects the measurement, it was carefully determined by first calculating the mass by measuring the size of the bead in a scanning electron microscope (see inset figure 1) and by applying the density given by the manufacturer. To validate the calculated bead mass, we used the established approach of measuring the resonance frequency shift of the fundamental out-of-plane mode in dependence of the attached mass (Dohn *et al* 2007). A set of six different cantilevers, ranging from 300 to 500 μm in length and from 50 to 75 μm in width, was prepared and the bead was successively transferred from one cantilever to another cantilever using a standard atomic force microscope (AFM) equipment. The frequency shift induced by the bead was measured, thus enabling to calculate and verify the previously determined bead mass $m_{\mathrm{Bead}} = 1.245 \pm 0.045$ ng.

The cantilever used for the investigation of the position-dependent mass responsivity of the fundamental roof tile-shaped mode was fabricated from a 4 inch

[4] Micromod Sicastar® ($\rho = 1.8\ \mathrm{g\ cm^{-3}}$), http://micromod.de

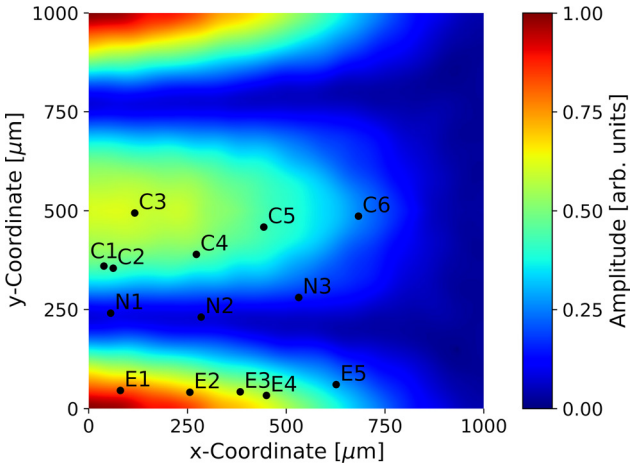

Figure 2. Distribution of the measured deflection across the surface of the cantilever, oscillating in the fundamental roof tile-shaped mode. The surface of the cantilever was scanned with a laser-Doppler vibrometer with a spatial resolution of approximately 13 μm. To plot the data a Gaussian filter and a cubic interpolation scheme was applied. The free end is located at $x = 0$ μm and the cantilever is fixed at $x = 1000$ μm. The highlighted points show the positions along the edge (E), on the nodal lines (N) and in the centre (C) where the mass responsivity $\mathcal{R}_{\mathrm{Meas}}$ was measured.

silicon-on-insulator wafer (figure 1). The (1 0 0)-orientated device layer had a thickness of 20 μm, defining the thickness of the cantilever. The device geometry (quadratic, side length: 1000 μm) was defined by structuring the device layer with a deep reactive ion etching (DRIE) process. Then, the cantilever was released by etching the handle layer with DRIE and subsequent removal of the buried oxide using hydrofluoric acid. A second cantilever of the same geometry and fixed to the same substrate served as a reference to cancel out any temperature effects, as explained below. The resonance frequency of the fundamental roof tile-mode for this device geometry is approximately 205 kHz in vacuum with a Q-factor of 8000. Figure 2 shows a laser-Doppler vibrometer scan of the displacement of the fundamental roof tile-shaped mode across the cantilever surface during oscillation.

The mass responsivity of a certain point on the cantilever surface was determined in multiple steps. First, the sample consisting of two identical cantilevers (here called *active* and *reference* cantilever) was placed in a vacuum chamber to eliminate any kind of external damping. A laser source was focused on the free end of the cantilevers and the power of the laser was modulated with a chirp signal bandwidth of 125 Hz to excite the fundamental roof tile-shaped mode (Ilic *et al* 2005). Note that in this first step, no mass is attached to the cantilevers. We then recorded the amplitude- and phase-spectra of both cantilevers using a laser-Doppler vibrometer (Polytec MSA-500). The phase response-function (Schmid *et al* 2016)

$$\varphi(\Omega) = \varphi_0 + \arctan \frac{2\zeta\left(\frac{\Omega}{\Omega_0}\right)}{\left(\frac{\Omega}{\Omega_0}\right)^2 - 1} \tag{1}$$

with the phase offset φ_0 and the damping ratio ζ was fitted to the data to determine the resonance frequency Ω_0, which is called $\Omega_{\mathrm{Act},0}$ for the 'active' cantilever with zero added mass and $\Omega_{\mathrm{Ref},0}$ for the reference cantilever. The standard deviation of ten subsequent measurements was 0.17 Hz.

In the second step, the previously characterised silicon dioxide bead was transferred to a predefined position on the *active* cantilever surface using the aforementioned AFM micromanipulation technique with a lateral precision of 2.5 μm. Figure 1 shows a confocal micrograph of the cantilever during the bead transfer process. Note, that no mass is attached to the reference cantilever. The measurement procedure as explained above is repeated, which results in the resonance frequencies $\Omega_{\mathrm{Act},1}$ and $\Omega_{\mathrm{Ref},1}$ for the mass-loaded active cantilever and reference cantilever, respectively.

In a last step, the mass responsivity is calculated for the respective position (x_i, y_i) on the cantilever surface by

$$\mathcal{R}_{\mathrm{Meas}}(x_i, y_i) = -\frac{\Delta\Omega}{m_{\mathrm{Bead}}}. \tag{2}$$

Since the resonance frequency is also influenced by changes of the temperature, we take the measurements of the reference cantilevers resonance frequency into account in order to eliminate these effects:

$$\Delta\Omega = (\Omega_{\mathrm{Act},1} - \Omega_{\mathrm{Act},0}) + (\Omega_{\mathrm{Ref},0} - \Omega_{\mathrm{Ref},1}). \tag{3}$$

We repeated this measurement procedure for fourteen different positions across the cantilever surface, which are highlighted in figure 2.

3. Results and discussion

3.1. Measurement results and verification

The measured mass responsivity values are given in the first row of table 1. Due to limited accuracy when determining the resonance frequency, the uncertainty of these values is 0.14 Hz ng^{-1}. Additionally, the limited accuracy in determining the bead mass accounts for a systematic error of approximately $\pm 3.5\%$. Note that due to the symmetry of the mode shape, it is sufficient to probe only one half of the cantilever. As already demonstrated for the flexural out-of-plane mode, the mass responsivity at a certain position on the cantilever surface is closely connected with the corresponding vibrational amplitude (Yu and Li 2009). The highest mass responsivity is found in the edge regions of the free end of the cantilever, where the bead gains high kinetic energy and therefore change the resonance frequency most significantly. On the other hand, the mass responsivity close to the nodal points is negligible, as the amplitude is close to zero in these areas.

In order to validate the measurements, FEA was conducted to calculate the eigenfrequency of the cantilever with an attached bead mass, while varying its position across the surface. The simulated resonance frequency shift was used to calculate the position-dependent mass responsivity of the FEA model $\mathcal{R}_{\mathrm{FEA}}$, which is given in the second row of table 1. A very good agreement with the measured values is found, whereas the largest relative deviations up to 60% are found in areas of low mass responsivity. Since the resonance frequency shift is well below 1 Hz at these positions, the limited

Table 1. The values of the experimentally determined mass responsivity $\mathcal{R}_{\mathrm{Meas}}$, the simulated values $\mathcal{R}_{\mathrm{FEA}}$ and the values of $\mathcal{R}_{\mathrm{Analytic}}$ as calculated by equation (6) for the positions highlighted in figure 2. The last row contains the maximal deviation of $\mathcal{R}_{\mathrm{Analytic}}$ for the assumed spatial error of 2.5 μm when determining the bead position. All values are in Hz ng^{-1}.

	Centre						Nodal lines			Edge				
Positions	C1	C2	C3	C4	C5	C6	N1	N2	N3	E1	E2	E3	E4	E5
$\mathcal{R}_{\mathrm{Meas}}$	3.90 (±0.28)	3.53 (±0.27)	6.78 (±0.39)	4.15 (±0.29)	3.84 (±0.28)	1.17 (±0.18)	0.11 (±0.14)	0.10 (±0.14)	0.60 (±0.16)	13.37 (±0.62)	10.31 (±0.51)	7.50 (±0.41)	6.10 (±0.36)	1.80 (±0.21)
$\mathcal{R}_{\mathrm{FEA}}$	3.50	3.24	6.76	3.96	3.90	1.17	0.04	0.04	0.49	13.49	10.10	6.76	5.79	1.50
$\mathcal{R}_{\mathrm{Analytic}}$	3.50	3.21	6.72	3.93	3.87	1.18	0.02	0.02	0.48	13.37	10.12	6.69	5.73	1.48
$\Delta\mathcal{R}_{\mathrm{max}}$	0.11	0.1	0.02	0.08	0.04	0.02	0.02	0.01	0.03	0.38	0.29	0.21	0.18	0.06
												(All values in Hz ng^{-1})		

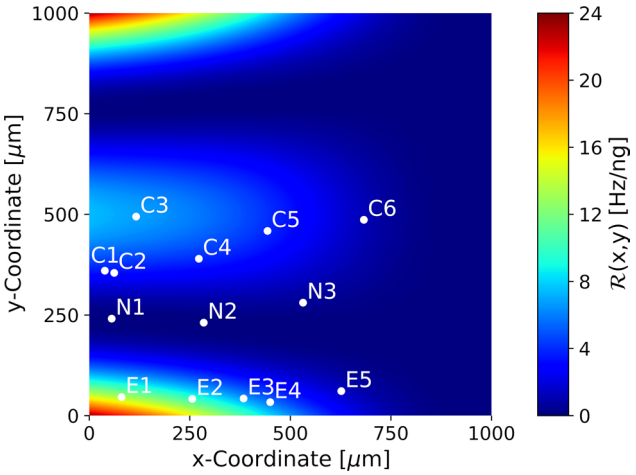

Figure 3. Surface plot of the analytically derived mass responsivity $\mathcal{R}_{\text{Analytic}}$ (equation (6)). The free end is located at $x = 0$ μm and the cantilever is fixed at $x = 1000$ μm. The values of $\mathcal{R}_{\text{Analytic}}$ at the highlighted points are given in the third row of table 1.

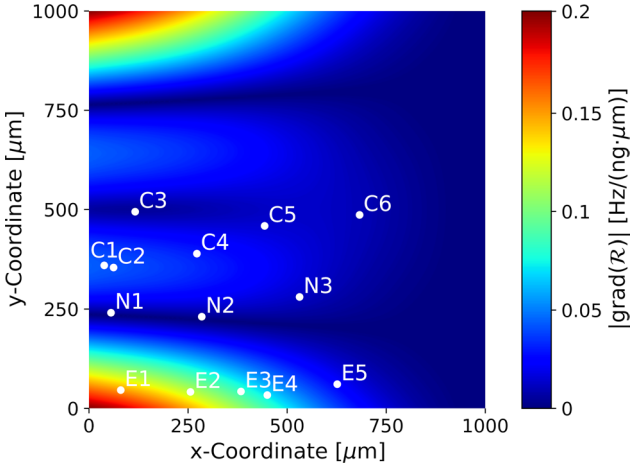

Figure 4. Gradient of the analytically derived mass responsivity. The free end is located at $x = 0$ μm and the cantilever is fixed at $x = 1000$ μm. The values at the highlighted positions are used to calculate the maximal deviation of $\mathcal{R}_{\text{Analytic}}$ for an error in lateral bead position of 2.5 μm.

accuracy of about 0.17 Hz when experimentally determining the resonance frequency introduces a significant error to the measurements, thus dominating the overall accuracy.

3.2. Spatial distribution of the mass responsivity

For mass sensing applications, it is desired to promote the accumulation of mass in regions with high mass responsivity. Thus, the spatial distribution of the mass responsivity is required to optimize the sensor design. The well-known formula for the resonance frequency of a cantilever, loaded with a point mass Δm at the position $x_{\Delta m}$ along the length is generalized to the 2D case (Dohn *et al* 2007):

$$\Omega_{\Delta m}^2 = \Omega_0^2 \left(1 + \frac{\Delta m}{m_c} \phi^2 \left(x_{\Delta m}, y_{\Delta m}\right)\right)^{-1}. \tag{4}$$

Here, m_c is the mass of the cantilever, Ω_0 is the resonance frequency without the point mass. Since it is assumed that the cantilever mass greatly exceeds the additional mass, a Taylor approximation for Δm leads to the final expression for the position-dependent mass responsivity of the 2D roof tile-shaped mode

$$\mathcal{R}_{\text{Analytic}}\left(x_{\Delta m}, y_{\Delta m}\right) = -\frac{\Omega_{\Delta m} - \Omega_0}{\Delta m} = -\frac{\Omega_0}{2m_c} \phi^2 \left(x_{\Delta m}, y_{\Delta m}\right). \tag{5}$$

For the flexural out-of-plane modes, an 1D expression of the mode shape function ϕ can be derived analytically (Schmid *et al* 2016). Up to date, such an expression is not available for the 2D roof tile-shaped mode. Because of the complex mode shape, simple approximations do not yield satisfactory results. Thus, we obtained the values of the mode shape function by a FEA: an eigenfrequency study of the microcantilever is performed and the values of the mode shape function are extracted from these simulation results. An anisotropic material model must be used, since the orientation-dependent mechanical properties of monocrystalline silicon have a strong impact on the derived mode shape in the case of 2D modes (Hopcroft *et al* 2010). Since the simulated mode shape is normalized in an arbitrary manner, a suitable normalization scheme has to be applied. The mass responsivity $\mathcal{R}_{\text{D}}$ of a cantilever, coated with an evenly distributed mass, is given by

$$\mathcal{R}_{\text{D}} = \frac{1}{LW} \int_0^L \int_0^W \mathcal{R}\left(x, y\right) \text{d}x\text{d}y = -\frac{1}{2} \frac{\Omega_0}{m_c} \tag{6}$$

with L and W being the length and width of the cantilever, respectively. By comparison to equation (5), it is obvious that the mode shape function $\phi(x, y)$ has to be normalized in a way that

$$\frac{1}{LW} \int_0^L \int_0^W \phi^2 \left(x, y\right) \text{d}x\text{d}y = 1\,. \tag{7}$$

The mode shape function, obtained by FEA, can now be used to calculate the mass responsivity at an arbitrary point (x, y) on the cantilever surface. A surface plot of $\mathcal{R}_{\text{Analytic}}$ as calculated by equation (5), is depicted in figure 3. To verify the validity of our expression, we calculated the values of $\mathcal{R}_{\text{Analytic}}$ at the previously measured positions, which are given in the third row of table 1 and compared them to $\mathcal{R}_{\text{Meas}}$. Excellent agreement is found, showing the validity of equation (5), which can now be used for further analysis of the position dependent mass responsivity.

Figure 3 shows that the highest mass responsivity is found at the edge regions at the free end of the cantilever with approximately 24 Hz ng^{-1}. As already mentioned in the introduction, our device has rather large geometrical dimensions in comparison to most resonant mass sensors found in literature, resulting in a high m_c value of about 50 μg. Despite this drawback, the mass responsivity in vacuum is comparable to devices of similar dimensions (Nugaeva *et al* 2007, Faegh *et al* 2013, Wasisto *et al* 2015). These studies utilise the flexural out-of-plane mode, where the high viscous damping of the out-of-plane modes renders their use in a liquid environment unfeasible (Manzaneque *et al* 2010). In contrast, the low viscous damping of the roof tile-shaped modes allows for the

utilisation of these class of modes for mass sensing applications in liquids (Patocka *et al* 2018).

3.3. Accuracy of mass determination

To determine the additional mass with high precision, its position on the cantilever surface has to be known precisely. To investigate the impact of limited spatial accuracy, we calculated the maximum error for our measurements due to a limited bead position measurement of 2.5 μm. First, we determined the magnitude of the gradient of $\mathcal{R}_{\text{Analytic}}$, as illustrated in figure 4, and calculated the resulting maximum error $\Delta\mathcal{R}_{\max}$ for all fourteen measurements, which is given in the fourth row of table 1. For most positions, the error is well below 5%, whereas it is significantly larger for the measurements next to the nodal lines. Despite the low gradient in these areas, the error has the same magnitude as the mass responsivity, thus making these areas less attractive for mass sensing purposes. Additionally, accumulation of matter in this area can counteract the mass-induced frequency shift by 'stiffening' the microcantilever (Tamayo *et al* 2006). To maximize the overall mass responsivity of the sensor, it should be avoided to accumulate any additional mass on or even close to the nodal lines. For the fundamental out-of-plane mode this effect is only relevant close to the anchor region of the cantilever, but special care has to be taken when designing a sensor exploiting the roof tile-shaped mode, as the nodal lines spread along the whole length of the cantilever. Even though the edge of the microcantilever exhibits the largest mass responsivity (position E1), the high gradient leads to a significant error even for small deviations of the assumed mass position. The lowest error is found for position C3 being in the centre of the cantilever. Since the gradient of the mass responsivity is close to zero in this area, inaccuracies when determining the mass position have a very low impact on the measurement, whereas the error when determining the resonance frequency shift can become prominent. Provided that the resonance frequency shift is significantly larger than the uncertainty when determining the resonance frequency (e.g. 0.17 Hz for our measurements), the added mass can be determined with the highest precision in this area.

4. Conclusions

By measuring the frequency shift induced by carefully placing a microbead on the cantilever, we determined the mass responsivity of the fundamental roof tile-shaped mode at distinct positions across the surface. The measurements show very good agreement with FEA and were used to verify an analytic expression for the position-dependent mass responsivity. We found a maximum mass responsivity of 24 Hz ng^{-1} at the edge regions of the cantilever. Given the large device size of $1000 \times 1000 \times 20$ μm^3, this shows the feasibility of our approach to use the fundamental roof tile-shaped mode for resonant mass sensing. Furthermore, we discussed the spatial distribution of the mass responsivity and identified the sources of errors when determining the added mass on the cantilever. Using this knowledge, the corresponding consequences for future sensor designs based on this vibrational mode were deduced. All in all, these promising results pave the way to study the mass sensing performance of higher orders of the roof tile-shaped modes even in liquid environments due to their high Q-factors.

Acknowledgments

This work was supported by the Austrian Research Promotion Agency within the 'Austrian COMET-Program' in the frame of K2 XTribology (project no. 849109). The authors acknowledge the TU Wien University Library for financial support through its Open Access Funding Programme.

ORCID iDs

F Patocka https://orcid.org/0000-0003-0197-1135

References

Buchapudi K R, Huang X, Yang X, Ji H-F and Thundat T 2011 Microcantilever biosensors for chemicals and bioorganisms *Analyst* **136** 1539–56

Cleveland J, Manne S, Bocek D and Hansma P 1993 A nondestructive method for determining the spring constant of cantilevers for scanning force microscopy *Rev. Sci. Instrum.* **64** 403–5

Cox R, Josse F, Heinrich S M, Brand O and Dufour I 2012 Characteristics of laterally vibrating resonant microcantilevers in viscous liquid media *J. Appl. Phys.* **111** 014907

Dohn S, Sandberg R, Svendsen W and Boisen A 2005 Enhanced functionality of cantilever based mass sensors using higher modes *Appl. Phys. Lett.* **86** 233501

Dohn S, Svendsen W, Boisen A and Hansen O 2007 Mass and position determination of attached particles on cantilever based mass sensors *Rev. Sci. Instrum.* **87** 103303

Dufour I, Heinrich S M and Josse F 2007 Theoretical analysis of strong-axis bending mode vibrations for resonant microcantilever (bio) chemical sensors in gas or liquid phase *J. Microelectromech. Syst.* **16** 44–9

Faegh S, Jalili N and Sridhar S 2013 A self-sensing piezoelectric microcantilever biosensor for detection of ultrasmall adsorbed aasses: theory and experiments *Sensors* **13** 6089–108

Hopcroft M A, Nix W D and Kenny T W 2010 What is the Young's modulus of silicon? *J. Microelectromech. Syst.* **19** 229–38

Ilic B, Krylov S, Aubin K, Reichenbach R and Craighead H 2005 Optical excitation of nanoelectromechanical oscillators *Appl. Phys. Lett.* **86** 193114

Johnson B N and Mutharasan R 2012 Biosensing using dynamic-mode cantilever sensors: a review *Biosens. Bioelectron.* **32** 1–18

Kucera M, Wistrela E, Pfusterschmied G, Ruiz-Díez V, Manzaneque T, Sánchez-Rojas J L, Schalko J, Bittner A and Schmid U 2014 Characterization of a roof tile-shaped out-of-plane vibrational mode in aluminum-nitride-actuated self-sensing micro-resonators for liquid monitoring purposes *Appl. Phys. Lett.* **104** 233501

Manzaneque T, Hernando J, Rodríguez-Aragón L, Ababneh A, Seidel H, Schmid U and Sánchez-Rojas J L 2010 Analysis of

the quality factor of AlN-actuated micro-resonators in air and liquid *Microsyst. Technol.* **16** 837–45
Nugaeva N, Gfeller K Y, Backmann N, Düggelin M, Lang H P, Güntherodt H-J and Hegner M 2007 An antibody-sensitized microfabricated cantilever for the growth detection of *Aspergillus niger* spores *Microsc. Microanal.* **13** 13–7
Oliver M, Hernando-García J, Ababneh A, Seidel H, Schmid U, Andrés J, Pobedinskas P, Haenen K and Sánchez-Rojas J L 2012 Resonantly excited AlN-based microcantilevers for immunosensing *Microsyst. Technol.* **18** 1089–94
Patocka F, Schlögl M, Schneider M and Schmid U 2018 Novel MEMS sensor for detecting magnetic particles in liquids *Proceedings* **2** 868
Pfusterschmied G, Kucera M, Wistrela E, Manzaneque T, Ruiz-Díez V, Sánchez-Rojas J L, Bittner A and Schmid U 2015 Temperature dependent performance of piezoelectric MEMS resonators for viscosity and density determination of liquids *J. Micromech. Microeng.* **25** 105014
Pfusterschmied G, Toledo J, Kucera M, Steindl W, Zemann S, Ruiz-Díez V, Schneider M, Bittner A, Sánchez-Rojas J L and Schmid U 2017 Potential of piezoelectric MEMS resonators for grape must fermentation monitoring *Micromachines* **8** 200
Schmid S, Villanueva L G and Roukes M L 2016 *Fundamentals of Nanomechanical Resonators* (Berlin: Springer)
Tamayo J, Ramos D, Mertens J and Calleja M 2006 Effect of the adsorbate stiffness on the resonance response of microcantilever sensors *Appl. Phys. Lett.* **89** 224104
Van Eysden C A and Sader J E 2007 Frequency response of cantilever beams immersed in viscous fluids with applications to the atomic force microscope: arbitrary mode order *J. Appl. Phys.* **101** 044908
Wasisto H S, Merzsch S, Uhde E, Waag A and Peiner E 2015 Partially integrated cantilever-based airborne nanoparticle detector for continuous carbon aerosol mass concentration monitoring *J. Sens. Sens. Syst.* **4** 111–23
Wasisto H S, Merzsch S, Waag A, Uhde E, Salthammer T and Peiner E 2013 Airborne engineered nanoparticle mass sensor based on a silicon resonant cantilever *Sensors Actuators* B **180** 77–89
Yu H and Li X 2009 Bianalyte mass detection with a single resonant microcantilever *Appl. Phys. Lett.* **94** 011901